Original Article

Sinogram-based coil selection for streak artifact reduction in undersampled radial real-time magnetic resonance imaging

H. Christian M. Holme[1], Jens Frahm[1,2]

[1]Max Planck Institute for Biophysical Chemistry, 37070 Göttingen, Germany; [2]DZHK (German Center for Cardiovascular Research), partner site Göttingen, Göttingen, Germany

Correspondence to: H. Christian M. Holme. Max Planck Institute for Biophysical Chemistry, 37070 Göttingen, Germany. Email: cholme@gwdg.de.

Background: Streak artifacts are a common problem in radial magnetic resonance imaging (MRI). We therefore developed a method for automatically excluding receiver coil elements which lead to these artifacts.

Methods: The proposed coil selection relates to real-time MRI data based on highly undersampled radial acquisitions. It exploits differences between high- and low-resolution sinograms reconstructed from datasets acquired during preparatory scans. Apart from phantom validations, the performance was assessed for real-time MRI studies of different human organ systems in vivo.

Results: The algorithm greatly reduces streak artifact strength without compromising image quality in other parts of the image. It is robust with respect to different experimental settings and fast to be included in the online reconstruction pipeline for real-time MRI.

Conclusions: The proposed method enables a fast reduction of streak artifacts in radial real-time MRI.

Keywords: Coil selection; streak artifacts; radial MRI; real-time MRI

Submitted Aug 02, 2016. Accepted for publication Sep 14, 2016.
doi: 10.21037/qims.2016.10.02
View this article at: http://dx.doi.org/10.21037/qims.2016.10.02

Introduction

Streak artifacts are a common problem in undersampled radial magnetic resonance imaging (MRI) (1). While even moderate undersampling can compromise image quality, the experimental settings for real-time MRI (2) exacerbate this problem. This is mainly because the degree of undersampling necessary for significantly reducing the acquisition time invariably emphasizes streak artifacts in the resulting images. Although most of these problems may effectively be mitigated by temporal regularization during nonlinear inverse (NLINV) reconstruction (2) or ameliorated by temporal median filtering afterwards, remaining artifacts arise from signal disturbances caused by magnetic field inhomogeneities or gradient nonlinearities or originate from off-resonance contributions of the object itself, e.g., due to pronounced fat signals or tissue susceptibility differences.

Coil selection has previously been applied to remove streak artifacts in radial MRI (3,4). These approaches rely on the assumption that streaks represent high-frequency objects in outer k-space, because, in radial sampling, the degree of undersampling increases with distance from the center of k-space. The algorithms assign a value for the strength of streak artifacts to each coil, either by using a difference image at high and low resolution or directly by using the difference in k-space. Coils are then sorted into two groups based on streak strength, and the group of high-streak strength is excluded from the reconstruction.

However, both methods have not been developed for the conditions of real-time MRI, which poses even more challenges: First, because online reconstruction is desired, the algorithm for coil selection needs to be very fast. And second, the high degree of undersampling leads to low overall signal strength. Therefore, the purpose of this work was to develop an advanced coil selection algorithm, which is especially suited for real-time MRI scenarios.

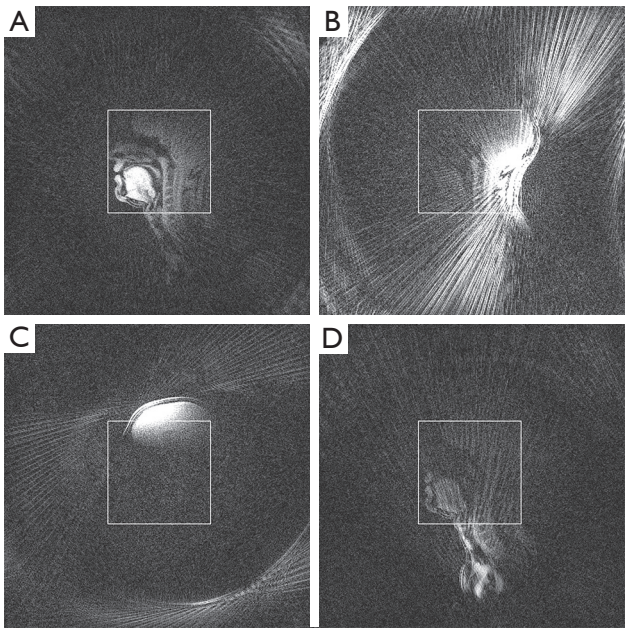

Figure 1 Selected single-coil images (same windowing) of an undersampled radial FLASH acquisition of a midsagittal section of the head using the standard 64-element head coil. (A) While some coils contain useful signal inside the indicated FOV; (B) others contain either streak artifacts; (C) provide signal intensity outside the FOV; or (D) contribute very little signal at all within the FOV. FOV, field of view; FLASH, fast low-angle shot.

Methods

The central insight justifying coil selection for streak artifact reduction is that only a subset of coils contains data responsible for streak artifacts in the reconstructed image. This can be seen by studying individual coil images, reconstructed with plain gridding and subsequent FFT-based reconstruction of individual coil data. *Figure 1* shows representative examples for different coil elements present in a typical acquisition: While some coils carry useful signal, other elements contribute almost no signal inside the field of view (FOV) or contain significant streak artifacts. Excluding the latter during reconstruction can greatly reduce or even remove these artifacts from the resulting image.

The proposed selection method, termed sinogram-based selection, is an extension of the algorithm by Grimm *et al.* (4), as it also exploits the difference between high- and low-resolution k-space data. However, because streak artifacts have a defined spatial origin, which cannot be identified in k-space, the proposed difference strategy is performed on sinograms which are obtained by 1D FFT of each radial k-space line and as such preserve spatial locality. This enables subsequent noise filtering to preserve the spatial streak origin while still reducing the influence of the low signal-to-noise ratio of a real-time acquisition.

Algorithm

In order to retain a sufficient number of coils for successful image reconstruction, the signal contribution of each coil to the final image is estimated, and coils are only removed up to a certain signal threshold. Furthermore, coils lacking any signal are identified and subsequently ignored in the algorithm. The general strategy of the algorithm is as follows:

- Step 1: for each coil n, take the ungridded raw k-space data h_n and generate a low-resolution variant l_n by assigning the inner $1/8^{\text{th}}$ of samples of h_n to l_n;
- Step 2: calculate the 1D FFT of h_n and l_n along the sample direction to obtain high- and low-resolution sinograms $s_{h,n}$ and $s_{l,n}$;
- Step 3: approximate the signal contribution F_n of each coil to the FOV by the L_2 norm of the inner part of the high-resolution sinogram. The width of this inner part is the length of the diagonal of the FOV (see indicated area in *Figure 2*). Normalize each F_n by dividing by $\sum_n F_n$;
- Step 4: calculate the mean μ_F and the standard deviation σ_F of the FOV contribution F_n. Any coil with $F_n < 1/3(\mu_F+\sigma_F)$ is ignored for the rest of the algorithm. Renormalize F_n for each coil;
- Step 5: calculate the magnitude of the complex difference $s_{diff,n} = |s_{h,n} - s_{l,n}|$, its standard deviation $\sigma_{diff,n}$ and its mean $\mu_{diff,n}$;
- Step 6: for each coil n, apply thresholding to $s_{diff,n}$ with threshold $T=\mu_{diff,n}+4\sigma_{diff,n}$, that means set $s_{diff,n}$ to zero where it is smaller than T, generating the thresholded $s^T_{diff,n}$;
- Step 7: calculate the streak ratio R_n for each coil as $R_n = \left\| s^T_{diff,n} / s_{l,n} \right\|$;
- Step 8: apply k-means (5) to sort the streak ratios into two groups clustered around two centers;
- Step 9: calculate the distance between the clustering centers. If it is less than twice the average standard deviation, repeat step 8 up to $n_{tries} = 100$ times;
- Step 10: if the combined FOV contribution of all coils in the high-streak group is more than 20% of the total signal, exclude the coils with the highest streak ratio until 20% excluded intensity is reached, otherwise exclude all coils in the high group.

Figure 2 illustrates the central steps of the proposed coil selection: The difference between the high- and low-resolution sinograms clearly identifies the streak origin, but it is contaminated by noise which is removed by the thresholding-based noise filter. The widths of the low-pass box filter in Step 1 and the threshold values have been determined empirically.

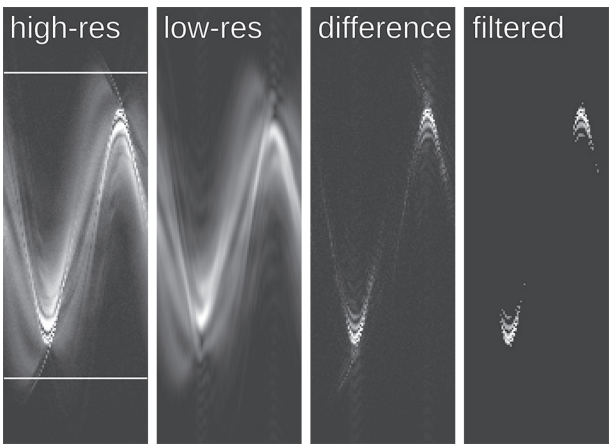

Figure 2 Sinograms of the single-coil data shown in *Figure 1B* illustrating the principle of sinogram-based coil selection. Because the difference between the high- and low-resolution sinogram is contaminated by noise, a thresholding-based noise filter is applied. The ratio of the norm of the filtered difference sinogram and the low-resolution sinogram is used as the streak ratio. The high-resolution sinogram indicates the area used to estimate the contribution of each coil to the FOV. FOV, field of view.

Evaluation

For evaluation of the algorithm, real-time MRI movies were reconstructed using NLINV (2) with either data from all coils or a subset of coils as obtained by sinogram-based selection. All reconstructions were performed using a Supermicro SuperServer 4027GR-TR system with the Ubuntu 14.04 operating system, 2x Intel Xeon Ivy Bridge E5-2650 main processors, 8x NVIDIA GTX Titan Black (Kepler GK110) GPUs as accelerators, and 128 GiB main memory. Coil selection was implemented as a preprocessing step using raw data of a few leading frames of a real-time acquisition. Because real-time image series typically employ multiple (here: 5) consecutive frames with complementary sets of spokes (2), coil selection takes advantage of a respective combined dataset. The selection is then applied to the entire movie. The images were visually inspected for the presence and strength of streak artifacts as no generally accepted criterion for quantification of image quality exists in MRI.

Four different acquisition modes, representing important applications of real-time MRI, were used for the evaluation of the proposed algorithm. All acquisition techniques rely on radial fast low-angle shot (FLASH) sequences with either refocusing gradients yielding T2/T1 contrast as used for dynamic monitoring of the temporomandibular joint (6) or random RF spoiling (7) for T1 contrast in studies of cardiac function (8), articulatory processes (9), and flow (10); for details see *Table 1*. All acquisitions used two-fold readout oversampling, which was removed by cropping after reconstruction. Reconstruction further involved a gradient delay correction,

Table 1 Acquisition parameters for real-time MRI

Contrast	Head		Heart	Phantom
	T1	T2/T1	T1	T1
Imaging time (ms)	33	60	18	40
Rate/frames (s^{-1})	30	17	55	25
Resolution (mm^3)	1.5×1.5×10	1.0×1.0×6	1.6×1.6×6	1.2×1.2×6
FOV (mm^2)	192×192	192×192	256×256	192×192
Reconstruction matrix (mm^2)	128×128	192×192	160×160	160×160
Acquired spokes	17	17	9	17
TR (ms)	1.96	3.53	2.0	2.32
TE (ms)	1.28	1.98	1.23	1.58
Flip angle/deg	5	35	8	8
Bandwidth (Hz $pixel^{-1}$)	1,860	870	1,490	1,565

MRI, magnetic resonance imaging; FOV, field of view.

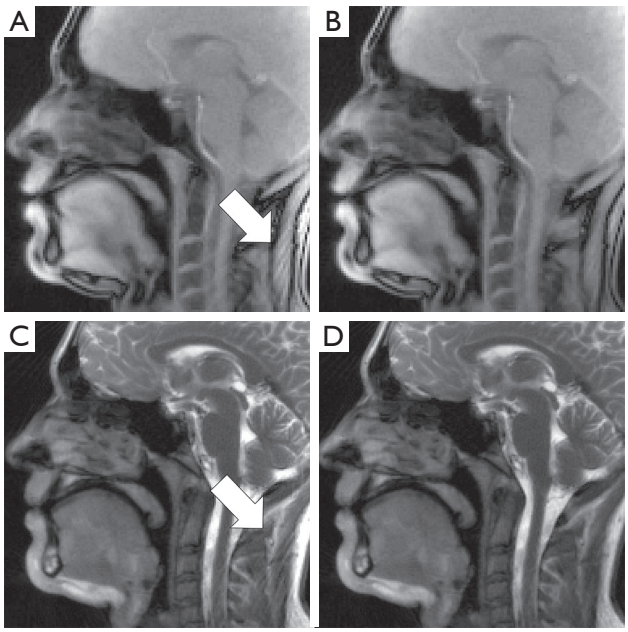

Figure 3 Representative frames of MRI movies of (A,B) spoiled and (C,D) refocused radial FLASH acquisitions of a midsagittal section through the head during speaking. (A,C) Reconstructions using all coils and (B,D) of a subset of coils after sinogram-based selection. Images using all coils show prominent streak artifacts (arrows) originating from the fat in the neck, whereas sinogram-based coil selection reduces the intensity of these artifacts greatly. MRI, magnetic resonance imaging; FLASH, fast low-angle shot.

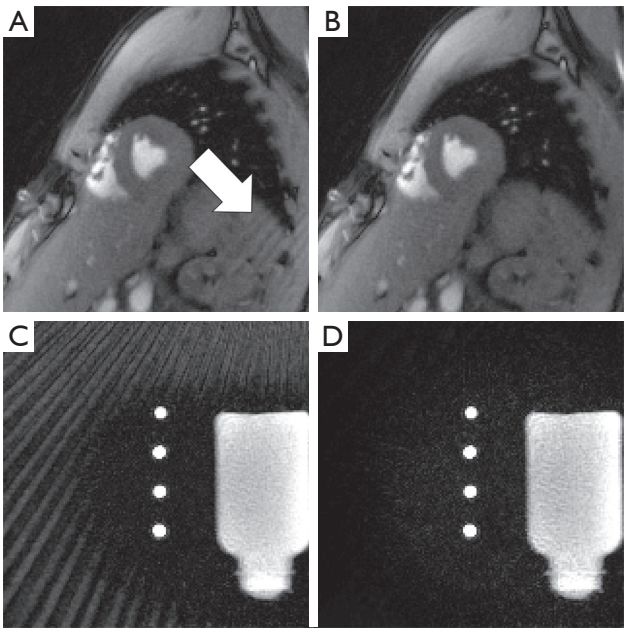

Figure 4 Representative frames of MRI movies of (A,B) a cardiac short-axis view and (C,D) a phantom with static water and perpendicular flow in four tubes. (A,C) Reconstructions using all coils and (B,D) of a subset of coils after sinogram-based selection. In the cardiac study streak artifacts originate from the shoulder. For the flow phantom, a larger tube with back flow above the actual FOV generates strong streak artifacts. In both cases, the artifact intensity is greatly reduced by sinogram-based coil selection. MRI, magnetic resonance imaging; FOV, field of view.

a compression to ten principal components (applied after coil selection) and gridding to a 1.5-times finer grid before using NLINV. A temporal median filter and a non-local means filter (11) were applied during post-processing.

MRI

All measurements were performed on a human MRI system operating at 3 T (Magnetom Prisma Fit, Siemens Healthcare, Erlangen, Germany) using either a 64-channel head coil or a combination of an 18-element thorax coil with suitable coils of the 32-element spine coil. Written informed consent according to the recommendations of the local ethics committee was obtained from all subjects prior to MRI.

Results

Figures 3 and *4* compare reconstructions using all coils with those of a subset of coils obtained by sinogram-based selection. The examples cover *in vivo* real-time MRI of the heart and head as well as of a flow phantom. In all cases, the use of all coils leads to visible streak artifacts. Their intensity is greatly reduced in images obtained by coil-selected reconstructions using the proposed method. Moreover, sinogram-based coil selection leaves image intensity and quality unaffected outside of the streak artifact regions. Runtime of the coil selection algorithm on the reconstruction system described above was below 0.5 s in all cases, with the majority of cases taking less than 0.1 s.

Discussion

Extending the idea of a previous approach for streak artifact reduction (4) to image space, the proposed sinogram-based method achieves rapid and efficient coil selection for real-time MRI using NLINV. The fast runtime below 0.5 s is sufficient to maintain real-time reconstruction, since the algorithm is only run once at the beginning of an acquisition. The new algorithm greatly reduces the

severity of streak artifacts and thereby improves the overall image quality both in phantoms and *in vivo*. Because affected coil elements are removed from the reconstruction, corresponding signal loss is confined to regions containing streak artifacts. Thus, the proposed algorithm leaves the image quality in other parts of the image uncompromised.

Because the sinogram-based coil selection relies on the k-means algorithm, it is not deterministic. Although numerous experimental applications proved considerable stability, individual datasets may show partially different selections on consecutive runs, which in turn may lead to non-reproducible reconstructions. Furthermore, since the streak ratios used in the algorithm are scalars, the k-means algorithm acts as a simple threshold. Thus, replacing the k-means algorithm by an appropriate threshold would lead to deterministic coil selection. So far, however, no such threshold has been found.

Another possible extension of the proposed algorithm is the generalization of coil selection to coil weighting. If streak artifacts mostly originate from high-intensity regions at the border or even outside the FOV, then weighting the coil contributions appropriately could lessen the severity of the residual artifacts, while still including potentially useful signal. Coil selection then emerges as a limiting case of coil weighting, where the coils are assigned binary weights.

Finally, in principle, regularization of the reconstruction method can be used to constrain the space of allowed solutions. It is therefore conceivable to design a regularization method which excludes images with strong streak artifacts from the solution space. This approach would completely negate the need for coil selection or coil weighting. But also in this respect, no methods have yet been found which reliably exclude streak artifacts from *in vivo* acquisitions.

Conclusions

In conclusion, sinogram-based coil selection has been shown to provide a simple and fast way to reduce streak artifacts in radial real-time MRI.

Acknowledgements

None.

Footnote

Conflicts of Interest: The authors have no conflicts of interest to declare.

References

1. Peters DC, Korosec FR, Grist TM, Block WF, Holden JE, Vigen KK, Mistretta CA. Undersampled projection reconstruction applied to MR angiography. Magn Reson Med 2000;43:91-101.
2. Uecker M, Zhang S, Voit D, Karaus A, Merboldt KD, Frahm J. Real-time MRI at a resolution of 20 ms. NMR Biomed 2010;23:986-94.
3. Xue Y, Yu J, Kang HS, Englander S, Rosen MA, Song HK. Automatic coil selection for streak artifact reduction in radial MRI. Magn Reson Med 2012;67:470-6.
4. Grimm R, Forman C, Hutter J, Kiefer B, Hornegger J, Block T. Fast automatic coil selection for radial stack-of-stars GRE imaging. Proc Intl Soc Magn Reson Med 2013;21:3786.
5. Hartigan JA, Wong MA. Algorithm AS 136: A K-Means Clustering Algorithm. J R Stat Soc C 1979;28:100-8.
6. Kling O, Rödiger M, Zhang S, Frahm J, Gersdorff N. Real-time MRI as a new technique for the functional assessment of the temporomandibular joint. J Craniomand Func 2013;5:9-18.
7. Roeloffs V, Voit D, Frahm J. Spoiling without additional gradients: Radial FLASH MRI with randomized radiofrequency phases. Magn Reson Med 2016;75:2094-9.
8. Zhang S, Joseph AA, Voit D, Schaetz S, Merboldt KD, Unterberg-Buchwald C, Hennemuth A, Lotz J, Frahm J. Real-time magnetic resonance imaging of cardiac function and flow-recent progress. Quant Imaging Med Surg 2014;4:313-29.
9. Niebergall A, Zhang S, Kunay E, Keydana G, Job M, Uecker M, Frahm J. Real-time MRI of speaking at a resolution of 33 ms: undersampled radial FLASH with nonlinear inverse reconstruction. Magn Reson Med 2013;69:477-85.
10. Untenberger M, Tan Z, Voit D, Joseph AA, Roeloffs V, Merboldt KD, Schätz S, Frahm J. Advances in real-time phase-contrast flow MRI using asymmetric radial gradient echoes. Magn Reson Med 2016;75:1901-8.
11. Klosowski J, Frahm J. Image Denoising for Real-Time MRI. Magn Reson Med 2016. [Epub ahead of print].

Cite this article as: Holme HCM, Frahm J. Sinogram-based coil selection for streak artifact reduction in undersampled radial real-time magnetic resonance imaging. Quant Imaging Med Surg 2016;6(5):552-556. doi: 10.21037/qims.2016.10.02